

Elimination of spiral chaos by periodic force for the Aliev-Panfilov model

Hidetsugu Sakaguchi and Takefumi Fujimoto

*Department of Applied Science for Electronics and Materials, Interdisciplinary Graduate School of Engineering Sciences,
Kyushu University, Kasuga, Fukuoka 816-8580, Japan*

(Received 4 February 2003; published 27 June 2003)

Spiral chaos appears in the two-dimensional Aliev-Panfilov model. The generation mechanism of the spiral chaos is related to the breathing instability of pulse trains. The spiral chaos can be eliminated by applying periodic force uniformly. The elimination of the spiral chaos is most effective when the frequency of the periodic force is close to that of the breathing motion.

DOI: 10.1103/PhysRevE.67.067202

PACS number(s): 05.45.Xt, 89.75.Kd, 87.19.Hh

Some types of cardiac arrhythmia are characterized by rotating waves that are similar to spiral waves found in excitable media [1]. Control and elimination of arrhythmia and the spiral waves are medically important. The control of regular spiral patterns in excitable media has been studied with several methods. Meandering of the spiral core can be controlled by a periodic parameter modulation [2]; impulses and periodic force have been applied to suppress spiral waves [3,4], and local and global feedback have been applied to excitable systems to eliminate spiral waves [5]. A serious cardiac arrhythmia, such as ventricular fibrillation, is related to the spiral chaos where many spiral cores are spontaneously generated. Eliminating the spiral chaos is more important.

Periodic forcing to spatio-temporal chaos was used to restore regular waves for diffusively coupled chemical oscillators and the complex Ginzburg-Landau equation [6,7]. In this Brief Report, we attempt to control and eliminate numerically the spiral chaos by applying a periodic force and find an effective frequency for the elimination. We use the following Aliev-Panfilov model for the cardiac cell [8]:

$$\begin{aligned} \frac{\partial e}{\partial t} &= -K(e-a)(e-1) - er + \nabla^2 e, \\ \frac{\partial r}{\partial t} &= [\epsilon + \mu_1 r / (\mu_2 + e)] [-r - ke(e-b-1)]. \end{aligned} \quad (1)$$

Here, e stands for the membrane potential and r stands for the conductance of the inward current. This model is a phenomenological model which represents certain feature of impulse propagation in a cardiac tissue. The parameter values of K , a , ϵ , μ_1 , μ_2 , and b are evaluated based on the real experiment. The model equation exhibits spiral breakup and spiral chaos in a certain parameter range [9].

We perform numerical simulations of Eq. (1). The parameters, except a , are fixed as $K=8$, $\epsilon=0.01$, $\mu_1=0.11$, $\mu_2=0.3$, and $b=0.1$. Firstly, we show numerical results for a one-dimensional system, that is, $\nabla^2 e$ in Eq. (1) is replaced by $\partial^2 e / \partial x^2$. The numerical simulation was performed using the finite difference method with $\Delta t=0.005$ and $\Delta x=0.5$. The system size L is 500, and the periodic boundary conditions are used. We have found that a pulse train propagates with a constant velocity for large a , however, the pulse train exhibits a breathing instability by decreasing a . Figure 1(a)

displays the time evolution of $e(x)$ at $a=0.063$ for the pulse train with wave number $k=2\pi(10/L)\sim 0.126$. The pulse width is temporally oscillating. The oscillatory instability of a single pulse in a one-dimensional ring of excitable media is called the alternans instability, since the pulse width almost alternates every time when the pulse turns around the ring [10]. The oscillatory instability of a pulse train with spatial period $2\pi/k$ almost corresponds to the alternans instability in a ring of size $2\pi/k$. The alternans instability in a ring of size $2\pi/k=L/10$ occurs as a supercritical Hopf bifurcation at $a=a_{c0}\sim 0.0647$. However, the oscillatory instability of the pulse train occurs at slightly larger $a=a_c\sim 0.0664$ for $k=2\pi(10/L)$ accompanying the spatial modulation. As seen in Fig. 1(a), the phase of the breathing motion is not synchronized for all pulses in the pulse train, as a result of the spatial modulation. As a is decreased further, the breathing amplitude becomes larger, and the spatial modulation grows. Finally, one pulse is annihilated and the wave number is decreased to $k=2\pi(9/L)$. The time evolution of the wave number decrease process is shown in Fig. 1(b) for $a=0.044$. It is characteristic of the cardiac tissue that the pulse width is easily varied with spatial periods of pulse trains. This characteristic is involved in the Aliev-Panfilov model. The critical parameters for the breathing instability and the wave number changing bifurcation strongly depend on the pulse interval. Figure 2 displays the two bifurcation curves (the breathing instability and the wave number decreasing bifurcation) as a function of wave number k . As the pulse interval $2\pi/k$ is narrower, the instabilities occur more easily, and the two bifurcation curves approach each other. The wave number changing process occurs just after the

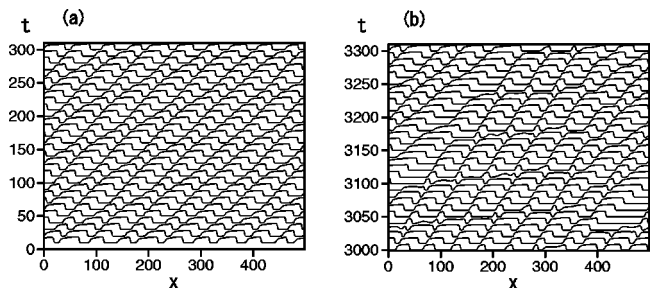


FIG. 1. (a) Time evolution of the breathing state at $a=0.063$ for the pulse train with wave number $k=2\pi(10/L)\sim 0.126$. (b) Time evolution of the wave number decrease process at $a=0.044$.

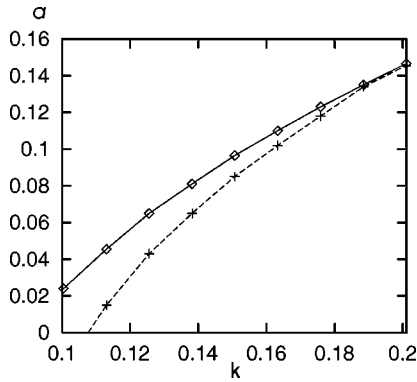


FIG. 2. Bifurcation curves as a function of wave number k of the pulse trains. The solid curve denotes the breathing instability, and the dashed curve denotes the bifurcation below which the wave number decreasing transition occurs.

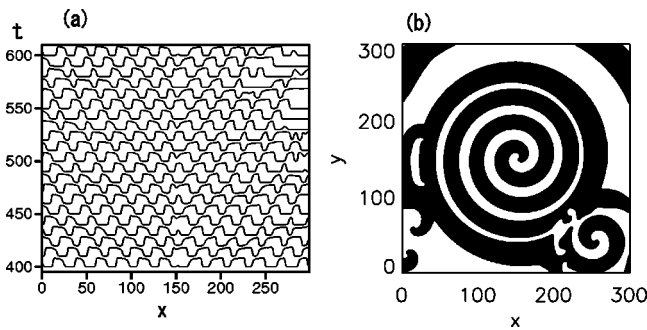


FIG. 3. Time evolution of $e(x, L-x)$ for $a=0.115$. The pulse trains emitted from the spiral core exhibit breathing motion and the pulse collapse occurs at $t \sim 520$. (b) Snapshot of e at $t=800$. In the shaded region, e is larger than 0.4.

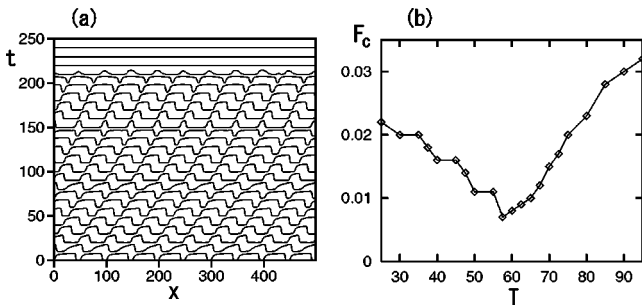


FIG. 4. (a) Time evolution for $a=0.06$, $k=2\pi(10/L)$, $F=0.009$, and $\omega=2\pi/60$. For $t > 220$, the pulse train is completely collapsed. (b) Critical values of F as a function of the period $T=2\pi/\omega$ of the external force for $a=0.06$.

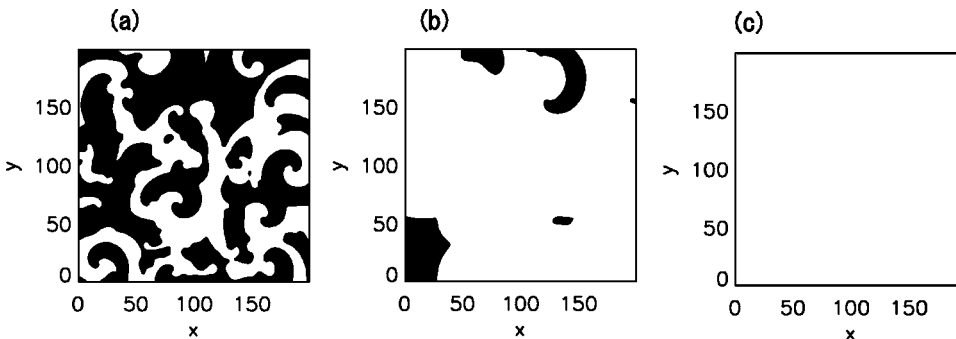


FIG. 5. Three snapshots of pattern of e at $t=0, 100$, and 300 for $a=0.1, F=0.036$, and $\omega=2\pi/60$. The spiral chaos disappears completely at $t=300$.

breathing instability for $k \sim 0.2$.

Next, we consider the instability of the spiral pattern in two dimensions. A stationary rotating spiral becomes unstable in a certain parameter range, as shown by Panfilov [9]. We have performed a numerical simulation of Eq. (1) in two dimensions. The system size is 300×300 and no flux boundary conditions are used. A spiral pattern is stable for $a > 0.13$ for the fixed parameters $K=8$, $\epsilon=0.01$, $\mu_1=0.11$, $\mu_2=0.3$, and $b=0.1$. The initial condition is a regular spiral pattern obtained numerically for $a=0.13$. Figure 3(a) displays a time evolution of $e(x,y)$ on line $y=L-x$ at $a=0.115$. At this parameter, pulse trains with wave number $k \sim 0.185$ are emitted from the spiral core. A one-dimensional pulse train with wave number $k \sim 0.185$ is unstable for the breathing motion at $a=0.115$, as is shown in Fig. 2. The pulse trains indeed exhibit breathing motion, and the wave number decreasing processes occur at $t \sim 520$. In one-dimensional system, the wave number decreasing process leads to a more stable structure with smaller wave number; however, in two dimensions, the wave number decreasing process leads to formation of additional topological defects, the spiral breaks up, and then spiral chaos appears. This is another route of spiral breakup, although it is similar to the spiral breakup via a wave number changing process by the Eckhaus instability [11]. Figure 4(b) displays a snapshot of e at $t=800$, where e takes a larger value than 0.4 in the shaded region. Two main spirals and several small spirals are generated as a result of the spiral breakup.

To eliminate the pulse train and the spiral chaos, we apply an external periodic force. The model equation is written as

$$\begin{aligned} \frac{\partial e}{\partial t} &= -k(e-a)(e-1) - er + \nabla^2 e + F \sin(\omega t), \\ \frac{\partial r}{\partial t} &= [\epsilon + \mu_1 r / (\mu_2 + e)] [-r - ke(e-b-1)], \end{aligned} \tag{2}$$

where F and ω are the amplitude and frequency respectively, of the external periodic force. We first show a numerical result of a one-dimensional system. Figure 4(a) displays a time evolution for $F=0.009$, $a=0.06$, $k=2\pi(10/L)$, and $\omega=2\pi/60$. The initial condition is a breathing state for Eq. (1), without the external force. The breathing motion of the pulse width is entrained to the external force. The amplitude of the breathing motion grows, and finally the pulse train structure collapses completely for $t > 230$. Thus, the pulse train could be eliminated by applying the external periodic

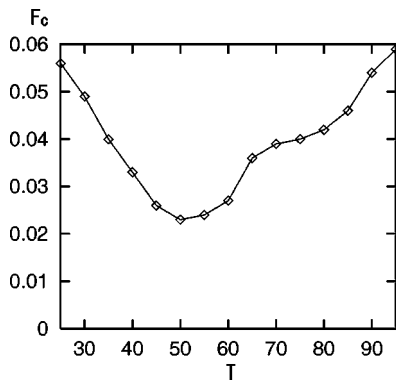


FIG. 6. Critical strength F for the spiral collapse at $a=0.1$ as a function of period T of the external force.

force. We have investigated a critical value of the amplitude F for the complete collapse. Figure 4(b) displays the critical values F_c as a function of period $T=2\pi/\omega$ for $a=0.06$. The phase diagram has a shape like the Arnold tongue for the forced entrainment, and the critical value F_c takes the smallest value at $T\sim 57.5$. The period is close to period $T'\sim 61$ of the natural breathing motion without the periodic forcing. These results are interpreted as a kind of resonance. That is, if the period of the external force is close to the period of the natural breathing motion, the effect of the external force is enhanced and the pulse train collapses easily.

We have applied a periodic force to eliminate the spiral chaos in two dimensions. The system size is 200×200 and

the value of parameter a is 0.1. The spiral chaos appears for this parameter. We have used a snapshot of the spiral chaos as an initial condition for the forced system. In the simulation of the two-dimensional system, we have applied the periodic force $F\sin\omega t$ to the spiral chaos only for $0 < t < 6\pi/\omega$ (three periods), and observed whether the spiral chaos collapses or the spiral chaos is maintained after the periods of the external forcing. The three periods are sufficient to see the effect of the external forcing. Figure 5 displays three snapshots of pattern of e at $t=0, 100$, and 300 for $a=0.1$, $F=0.036$, and $\omega=2\pi/60$. The spiral chaos collapses completely and the uniform state $e(x,y)=0$ and $r(x,y)=0$ have been obtained after the application of external force. We have numerically obtained the critical value F_c for the collapse of the spiral chaos. The critical strength F_c is shown in Fig. 6 as a function of the period $T=2\pi/\omega$. The critical curve takes minimum at $T\sim 50$. It is close to the period ~ 55 of the natural breathing motion at this parameter.

To summarize, we have performed numerical simulations of the Aliev-Panfilov model. We have found a breathing instability for the pulse trains in one dimension. The breathing instability leads to spiral breakup in two dimensions. The periodic force is applied to eliminate the pulse trains and the spiral chaos. We have found that the most effective frequency to eliminate the wave patterns is close to the natural frequency of the breathing motion. This is interpreted as a kind of the resonance effect. The periodic forcing with the most effective frequency may be effective as a method of mild defibrillation.

-
- [1] F.X. Witkowski, L.J. Leon, P.A. Penkoske, W.R. Giles, M.L. Spano, W.L. Ditto, and A.T. Winfree, *Nature (London)* **392**, 78 (1998).
 - [2] O. Steinbock, V. Zykov, and S.C. Müller, *Nature (London)* **366**, 322 (1993).
 - [3] G.V. Osipov and J.J. Collins, *Phys. Rev. E* **60**, 54 (1999).
 - [4] H. Sakaguchi and T. Fujimoto, *Prog. Theor. Phys.* **108**, 241 (2002).
 - [5] A.V. Panfilov, S.C. Müller, V.S. Zykov, and J.P. Keener, *Phys. Rev. E* **61**, 4644 (2000).
 - [6] G. Baier, S. Sahle, Y. Chen, and T. Hoff, *J. Chem. Phys.* **110**, 3251 (1999).
 - [7] H. Zhang, B. Hu, G. Hu, Q. Ouyang, and J. Kurths, *Phys. Rev. E* **66**, 046303 (2002).
 - [8] R.R. Aliev and A.V. Panfilov, *Chaos, Solitons Fractals* **7**, 293 (1996).
 - [9] A.V. Panfilov, *Phys. Rev. Lett.* **88**, 118101 (2002).
 - [10] M. Courtemanche, L. Glass, and J.P. Keener, *Phys. Rev. Lett.* **70**, 2182 (1993).
 - [11] M. Bär and M. Or-Guil, *Phys. Rev. Lett.* **82**, 1160 (1999).